

AN EVALUATION OF COMPRESSION-PERMEABILITY CHARACTERISTICS IN THE INTERMEDIATE CONCENTRATION RANGE BY USE OF CENTRIFUGAL AND CONSTANT-RATE COMPRESSION TECHNIQUES

TOSHIRO MURASE, MASASHI IWATA, TAKEHITO ADACHI,
LECH GMACHOWSKI, AND MOMPEI SHIRATO

*Department of Chemical Engineering, Nagoya University,
Nagoya 464-01*

Key Words: Solid Liquid Separation, Compression, Permeability, Centrifugal, Constant Rate, Zinc Oxide, Ferric Oxide

The compression-permeability characteristics of a solid-liquid mixture can be obtained from the gravitational sedimentation test (in dilute region) and the C-P cell method (in concentrated region). In this paper, two new methods—the centrifugal method for the compression data and the constant-rate compression method for the permeability data—to obtain the characteristics in the intermediate concentration region between the two are presented. In the centrifugal test, the compression data in the intermediate region can be obtained by choosing suitable centrifugal acceleration and measuring the equilibrium height of a sediment. The data are in good agreement with those in the concentrated region. The gravitational sedimentation data, however, show higher porosity because of the friction between the sediment and the inner wall of a cylinder. In the constant-rate compression test, a material is compressed in a C-P cell for a given time at the rate at which the material is kept approximately homogeneous, followed by the permeability measurement. The permeability data based on this method can be combined with C-P cell data and the sedimentation data of an extremely dilute suspension.

Introduction

Compression-permeability characteristics of a particulate layer are essential to the design of equipment for settling, sedimentation, filtration, expression, etc. of a solid-liquid mixture. If the mixture is sufficiently thick, the conventional compression-permeability cell (C-P cell) method,^{3,10)} the filtration method,⁴⁾ or the constant-pressure expression method⁵⁾ can be used to

obtain its compression-permeability data (C-P data). On the other hand, if the mixture is considerably dilute and fluid, the C-P data have been obtained only from the gravitational sedimentation test.^{8,11)} In general, a solid-compressive pressure in the sedimentation test is 2–3 orders smaller than that in the C-P cell method, although an understanding of the intermediate region between the dilute and the concentrated ones is important in the field of coagulation, flocculation and thickening.

Buscall²⁾ and Sambuichi, Nakakura *et al.*⁶⁾ developed the centrifugal sedimentation method for

Received September 2, 1988. Correspondence concerning this article should be addressed to T. Murase. L. Gmachowski is at Institute of Physical Chemistry, Polish Academy of Sciences, 01-224 Warsaw, Poland. M. Shirato is at Nagoya Industrial Science Research Institute, Nagoya 468.

obtaining the relationship between the average solid compressive pressure and the average porosity of a sediment. In this paper, a new method which also utilizes a centrifugal field is presented for obtaining a local compression characteristic of the mixture in the intermediate concentration range.

Furthermore, it is shown that the constant-rate compression technique^{1,7)} is useful for obtaining the permeability data in the intermediate region. A method for determining the compression rate under which the material is approximately homogeneous is presented.

1. Experimental Material and Procedure

Fine particulate zinc oxide and ferric oxide slurries were used as experimental materials. Their properties are listed in Table 1.

For the measurement of a compressibility by the centrifugal sedimentation method, a centrifugal tube with an inner diameter of 33 mm and a depth of 80 mm was used. The tube was spun in a centrifuge with an arm length R of 233 mm with the rotational speed N of 300–1000 r.p.m. for 120 min. Then, the thickness of the sediment was measured. It was confirmed that the thickness of the sediment became almost constant within 60 min since the operation was started.

A compression permeability cell (C-P cell) with an inner diameter of 60 mm was used for the constant-rate compression test. In the test, sediments prepared by gravitational settling were used as the material. The piston of the C-P cell was fixed at the cross-head of a material testing machine and lowered for a given time at a constant rate to compress the solid-liquid mixture in the cell. Thereafter, the movement of the piston was stopped and the permeability was measured by percolating the liquid through the material. The porosity of the material was calculated from its thickness.

For comparison with the data above, a gravitational sedimentation experiment^{8,11)} and a C-P cell test^{3,10)} were conducted. In the sedimentation test, a glass tube with an inner diameter of 62 mm was used. The permeability was calculated from the initial settling velocity of a suspension, while the compression datum was obtained from the equilibrium height of the sediment. In the C-P cell test, a constant pressure was applied to the cell with an inner diameter of 60 mm, resulting in a homogeneous semisolid material. The permeability was calculated from the percolation rate of a liquid and the porosity was calculated from its thickness.

The total solid volume per unit cross-sectional area of the cell ω_0 was as follows: $\omega_0 = 0.20$ – 0.35 cm in the centrifugal test; 0.30 – 0.32 cm in the constant-rate compression and the C-P cell tests; and 0.16 – 0.61 cm in the gravitational sedimentation test.

Table 1. Properties of experimental materials

		Zinc oxide	Ferric oxide
Particle density* ρ_s	[kg/m ³]	5.64×10^3	5.16×10^3
Specific surface area**	[m ² /m ³]	1.92×10^7	3.91×10^6
Specific surface diameter	[m]	0.31×10^{-6}	1.53×10^{-6}
E	[Pa ⁻¹]	0.0304	0.140
β	[—]	0.174	0.0816
e_0	[—]	18.4	5.03
C_c	[—]	1.38	0.286

* Obtained by air comparison pycnometer.

** Obtained by air permeability test.

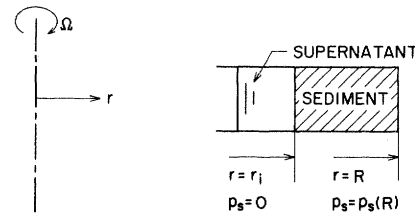


Fig. 1. Schematic illustration of the centrifugal test

2. Compression Characteristic in the Centrifugal Field

Figure 1 shows a sediment of equilibrium thickness in a centrifugal tube. The force balance for an infinitesimal layer in the sediment can be written as

$$\frac{dp_s}{dr} = (\rho_s - \rho)(1 - \varepsilon)r\Omega^2 \quad (1)$$

where p_s is the local solid compressive pressure; ε , the local porosity of the sediment; ρ_s and ρ , the true density of the solid and liquid, respectively; and Ω , the angular velocity of the centrifuge. From Eq. (1), Buscall²⁾ and Sambuichi, Nakakura *et al.*⁶⁾ derived the relation between the average porosity and average solid compressive pressure of the sediment. Here, we will discuss a technique for obtaining the local ε – p_s relationship of the material. Integration of Eq. (1) with respect to r yields the solid compressive pressure at the bottom of the tube, $p_s(R)$.

$$p_s(R) = (\rho_s - \rho)\Omega^2 \int_{r_i}^R (1 - \varepsilon)r dr \quad (2)$$

If $R \gg (R - r_i)$, the variable r in Eq. (2) can be approximated by $(R + r_i)/2$. Thus,

$$\begin{aligned} p_s(R) &= (\rho_s - \rho)\Omega^2 \frac{R + r_i}{2} \int_{r_i}^R (1 - \varepsilon) dr \\ &= (\rho_s - \rho)\Omega^2 \frac{R + r_i}{2} \omega_0 \end{aligned} \quad (3)$$

where ω_0 is the total solid volume per unit cross-sectional area of the tube. By choosing suitable Ω and ω_0 values, $p_s(R)$ corresponding to the intermediate concentration region can be obtained.

In general, the local compression characteristic of a mixture has been represented in the following forms.^{13,14)}

$$\left. \begin{aligned} 1 - \varepsilon &= E p_s^\beta & p_s \geq p_{si} \\ 1 - \varepsilon &= E p_{si}^\beta & p_s \leq p_{si} \end{aligned} \right\} \quad (4-a)$$

$$\left. \begin{aligned} e &= e_0 - C_c \ln p_s & p_s \geq p_{si} \\ e &= e_0 - C_c \ln p_{si} & p_s \leq p_{si} \end{aligned} \right\} \quad (4-b)$$

where e is the local void ratio ($e = \varepsilon / (1 - \varepsilon)$); and E , β , e_0 and C_c are empirical constants. p_{si} is the solid compressive pressure below which the local porosity is constant. A compression characteristic of any material may be represented by either or both of these equations.

When the above empirical constants (E , β , e_0 and C_c) are obtained, we can use the local compression characteristics Eqs. (4-a) or (4-b) for designing a solid-liquid separation operation. In the following, we will describe how to determine these empirical constants from the overall centrifugal data (sediment height $(R - r_i)$ vs. centrifugal acceleration $(R\Omega^2)$).

If the compression characteristics is represented by Eq. (4-a), combining Eqs. (1) and (4-a) and integrating Eq. (1) over the entire sediment one obtains

$$\int_0^{p_{si}} \frac{dp_s}{E p_{si}^\beta} + \int_{p_{si}}^{p_s(R)} \frac{dp_s}{E p_s^\beta} = (\rho_s - \rho) \Omega^2 \int_{r_i}^R r dr \quad (5)$$

Thus,

$$\frac{p_{si}^{1-\beta}}{E} + \frac{p_s(R)^{1-\beta} - p_{si}^{1-\beta}}{E(1-\beta)} = (\rho_s - \rho) \Omega^2 \frac{R + r_i}{2} (R - r_i) \quad (6)$$

Combining Eqs. (3) and (6) yields the $(R - r_i) - R\Omega^2$ relation

$$\begin{aligned} R - r_i &= \frac{\omega_0^{1-\beta}}{E(1-\beta)} \left\{ (\rho_s - \rho) \frac{R + r_i}{2} \Omega^2 \right\}^{-\beta} \\ &\quad - \frac{\beta p_{si}^{1-\beta}}{E(1-\beta)} \left\{ (\rho_s - \rho) \frac{R + r_i}{2} \Omega^2 \right\}^{-1} \\ &\doteq \frac{\omega_0^{1-\beta}}{E(1-\beta)} \{ (\rho_s - \rho) R \Omega^2 \}^{-\beta} \\ &\quad - \frac{\beta p_{si}^{1-\beta}}{E(1-\beta)} \{ (\rho_s - \rho) R \Omega^2 \}^{-1} \end{aligned} \quad (7)$$

If $R \gg (R - r_i)$, $(R + r_i)/2$ can be approximated by R in Eq. (7). As described later, the second term of the right-hand side of Eq. (7) is negligible. Thus, using Eq. (7) and plotting $(R - r_i)$ vs. $R\Omega^2$ on logarithmic paper, one can accordingly determine the values of E and β in Eq. (4-a).

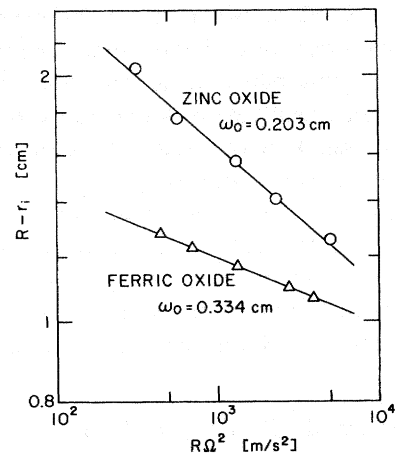


Fig. 2. $\ln(R - r_i)$ vs. $\ln(R\Omega^2)$

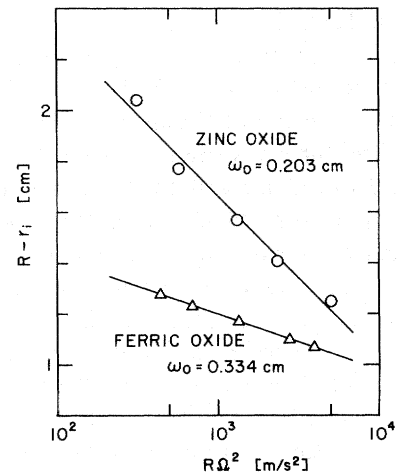


Fig. 3. $(R - r_i)$ vs. $\ln(R\Omega^2)$

If the local void ratio e of the mixture is represented by Terzaghi-Peck's form of Eq. (4-b), substituting Eq. (4-b) into Eq. (1) and integrating Eq. (1) over the entire sediment yield the following equation.

$$\begin{aligned} p_s(R) \{ 1 + e_0 + C_c - C_c \ln p_s(R) \} - C_c p_{si} \\ = (\rho_s - \rho) \Omega^2 \frac{R + r_i}{2} (R - r_i) \end{aligned} \quad (8)$$

Combining Eqs. (3) and (8) and letting $(R + r_i)/2 \doteq R$, one obtains another $(R - r_i) - R\Omega^2$ relation:

$$\begin{aligned} R - r_i &= (1 + e_0 + C_c) \omega_0 - C_c \omega_0 \ln \{ (\rho_s - \rho) \omega_0 R \Omega^2 \} \\ &\quad - \frac{C_c p_{si}}{(\rho_s - \rho) R \Omega^2} \end{aligned} \quad (9)$$

In this case, the third term of the right-hand side of Eq. (9) is also negligible, as shown later. Therefore, plotting $(R - r_i)$ vs. $R\Omega^2$ on semi-logarithmic paper, one can obtain the empirical constants e_0 and C_c in Eq. (4-b).

Figures 2 and 3 represent the results of the centrifugal test. Good linear relations are obtained for

$\ln(R-r_i)$ vs. $\ln(R\Omega^2)$ in Fig. 2 and for $(R-r_i)$ vs. $\ln(R\Omega^2)$ in Fig. 3. This implies that the terms which involve p_{si} in Eqs. (7) and (9) are both quite small compared with the others. Therefore, the values of E , β , e_0 and C_c can be determined from the figures. That is, both Eqs. (4-a) and (4-b) are usable for these materials in the pressure range of the centrifugal test. The values of E , β , e_0 and C_c appear in Table 1.

Figures 4 and 5 show the $(1-\varepsilon)-p_s$ relations and the $e-p_s$ relations, respectively. In the figures, the solid lines are the results of the centrifugal tests, and the broken lines represent the gravitational sedimentation characteristics.

In Fig. 4, the solid line based on Eq. (4-a) is in good agreement with the compression data in the concentrated region (C-P cell data). The gravitational sedimentation test corresponds to the case of $R\Omega^2 = (\text{gravitational acceleration})$ in the centrifugal test. However, the gravitational sedimentation line in the figure shows somewhat lower value than those extrapolated from others. This means that in the gravitational sedimentation test the effect of friction between the sediment and the inner wall of the cylinder is greater than in the other tests.

As shown in Fig. 5, solid lines based on Eq. (4-b) are also well located. However, the equation cannot be used over the entire concentration range for these materials because the data do not have a linear relation over such a wide range. Discontinuity between the broken and the solid lines can also be seen in Fig. 5.

3. Measurement of Permeability by Use of Constant-rate Compression Technique

To obtain the permeability data of a solid-liquid mixture in the intermediate concentration range, it is essential to prepare a stationary layer of the mixture with controlled thickness. Banks and Burton¹⁾ measured the permeability characteristic of brown coal by using the constant-rate compression method. In the experiment, the coal was compressed in a C-P cell at a constant rate for a fixed time. Then, the movement of the piston was stopped and the permeability of the sample was measured after allowing sufficient time for stress relaxation. In the present study, this method is applied for the intermediate concentration range. Here, the accuracy of the permeability measured depends on the degree of uniformity of the mixture. In Fig. 6, the results of the constant-rate compression test are shown together with the result of the C-P cell test. In the figure, α denotes the specific resistance and q is the compression rate, i.e. the dewatering rate per unit cross-sectional area of the filter medium. It can be seen from the figure that the $\ln \alpha - \ln(1-\varepsilon)$ relation converges to a linear relation and shows better correlation with the

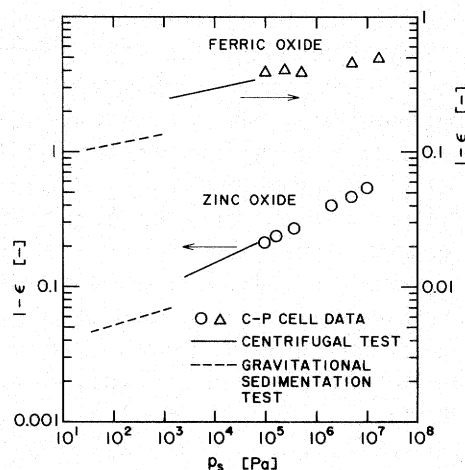


Fig. 4. Compression data, $(1-\varepsilon)$ vs. p_s

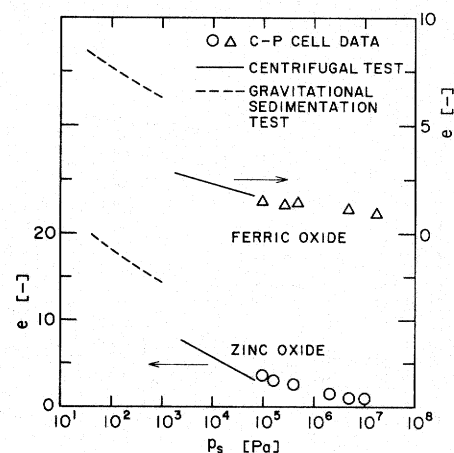


Fig. 5. Compression data, e vs. p_s

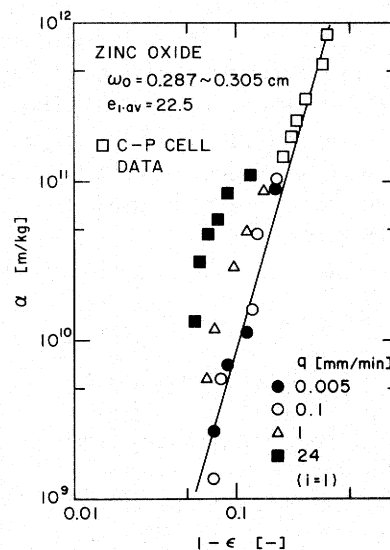


Fig. 6. Effect of compression rate q on α vs. $(1-\varepsilon)$ data

C-P cell data as q becomes smaller. Thus, one can deduce that a zinc oxide suspension compressed below the rate $q=0.1$ mm/min is almost homogeneous. In the following, we will describe how to determine the

compression rate under which the mixture prepared is approximately homogeneous.

In the previous paper, concerned with a constant-rate expression,^{1,2)} it was shown that the instantaneous expression rate is uniquely determined only by the instantaneous expression pressure p and the amount of removed liquid at the moment, and is not related to the pressure history. Consequently, the relation between p and the decrease of average void ratio ($-\Delta e_{av}$) (which represents the amount of the removed liquid) in the constant-rate expression can be found by using the equation for the constant-pressure expression.

If the creep effect of a material is negligible, ($-\Delta e_{av}$) and its time derivative ($-de_{av}/d\theta'_c$) (which represents the instantaneous expression rate) in a constant-pressure expression of a homogeneous material are represented as follows:^{1,2)}

$$-\Delta e_{av} = -\Delta e_{av,\infty} \left[1 - \sum_{N=1}^{\infty} \frac{8}{(2N-1)^2 \pi^2} \times \exp \left\{ -\frac{(2N-1)^2 \pi^2}{4} T'_c \right\} \right] \quad (10)$$

$$-\frac{\omega_0^2}{i^2} \frac{de_{av}}{d\theta'_c} = -2\Delta e_{av,\infty} C_e \times \sum_{N=1}^{\infty} \exp \left\{ -\frac{(2N-1)^2 \pi^2}{4} T'_c \right\} \quad (11)$$

where

$$T'_c = \frac{i^2 C_e \theta'_c}{\omega_0^2} \quad (12)$$

θ'_c is the consolidation time in the constant-pressure operation, and i means the number of drainage surfaces of the C-P cell. ($-\Delta e_{av,\infty}$) in Eqs. (10) and (11) is the total decrease of the average void ratio when the final equilibrium compression is attained under the constant pressure p , and it is represented in the following forms.

i) If the compression characteristic is represented by Eq. (4-a),

$$-\Delta e_{av,\infty} = \frac{1}{E} \{ p_s(e_{1,av})^{-\beta} - p^{-\beta} \} \quad (13-a)$$

ii) If it is represented by Eq. (4-b),

$$-\Delta e_{av,\infty} = C_e \ln \left\{ \frac{p}{p_s(e_{1,av})} \right\} \quad (13-b)$$

where $p_s(e_{1,av})$ is the solid compressive pressure corresponding to the average void ratio $e_{1,av}$ of the original mixture. C_e in Eqs. (11) and (12) is the average modified consolidation coefficient defined by

$$C_e = \frac{1}{\mu p_s \alpha_{av} (-de/dp_s)_{av}} \quad (14)$$

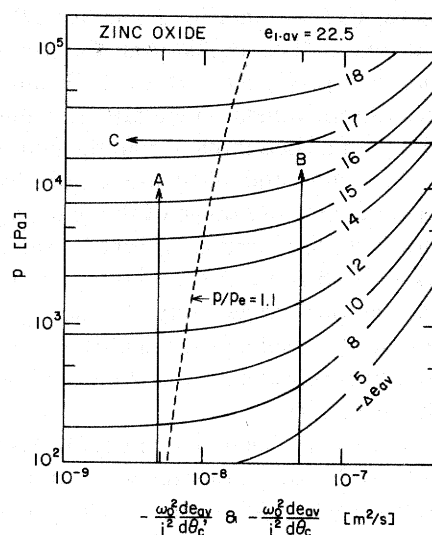


Fig. 7. Relationship among p , $(-\Delta e_{av})$ and $(-\omega_0^2/i^2 \cdot de_{av}/d\theta'_c)$ and $-\omega_0^2/i^2 \cdot de_{av}/d\theta'_c$ for ZnO mixture

where α_{av} and $(-de/dp_s)_{av}$ mean the average specific resistance and the average compressibility coefficient of the mixture, respectively. They correspond to the average solid compressive pressure $p_{s,av}$, which is the logarithmic mean value of $p_s(e_{1,av})$ and p .

Using the compression characteristics (Eq. (4-a)) and the approximate permeability data extrapolated from C-P cell data in the concentrated region, one can obtain the relationship among p , $(-\Delta e_{av})$ and $(-\omega_0^2/i^2 \cdot de_{av}/d\theta'_c)$ from Eqs. (10) and (11), as shown in Fig. 7. The operation line of the constant-rate compression at a given expression rate can be depicted as line A ($q=0.1$ mm/min in Fig. 6) or B ($q=1$ mm/min) shown in the figure,^{1,2)} while compression under a constant pressure proceeds along line C. θ'_c in Fig. 7 is the consolidation time in the constant-rate expression operation. In the constant-pressure compression, $(-\omega_0^2/i^2 \cdot de_{av}/d\theta'_c)$ approaches zero as compression proceeds and the compressed material becomes homogeneous. In the limit $(-\omega_0^2/i^2 \cdot de_{av}/d\theta'_c) \rightarrow 0$, the curves in the figure become horizontal, where the relation between p and $(-\Delta e_{av})$ coincides with that at the equilibrium compression state (p vs. $(-\Delta e_{av,\infty})$), which is represented by Eq. (13-a) or (13-b). Consequently, in the constant-rate compression a compressed material based on line A in the figure is more homogeneous than that based on line B at the same $(-\Delta e_{av})$. This can be confirmed by Fig. 8, which shows the results of numerical calculation for the constant-rate compression.⁹⁾ Here ω is the net solid volume per unit medium area lying from the medium up to an arbitrary position in the material ($i\omega/\omega_0=0$ at the filter medium, and $i\omega/\omega_0=1.0$ at the impermeable wall).

The broken line in Fig. 7 is the line of $p/p_e=1.1$, where p_e denotes the equilibrium pressure at a

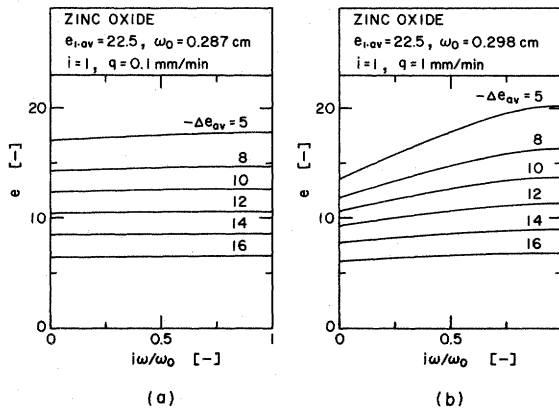


Fig. 8. Distribution of void ratio e during compression process. (a) and (b) are based on lines A and B respectively in Fig. 7

horizontal level in the figure calculated by

$$p_e = \{-E(-\Delta e_{av}) + p_s(e_{1,av})^{-\beta}\}^{-1/\beta} \quad (15-a)$$

(from Eq. (4-a))

$$\text{or} \quad p_e = p_s(e_{1,av}) \exp(-\Delta e_{av}/C_c) \quad (15-b)$$

(from Eq. (4-b))

(Under the constant pressure p_e , although it takes infinite time to compress the material until reaching $(-\Delta e_{av})$ in Eq. (15), the material is homogeneous when such $(-\Delta e_{av})$ is attained.) If the material is compressed at a rate on the left of the broken line in Fig. 7, its deviation from homogeneity is within 10% in regard to the solid compressive pressure, and hence p/p_e could be a measure of the deviation from the equilibrium compression. This can be the theoretical background of the constant-rate compression method.

In Figs. 9 and 10, the specific resistance α vs. the solidosity (packing fraction) $(1-\epsilon)$ obtained from the constant-rate compression test are illustrated together with the C-P cell data and the gravitational sedimentation data. For both figures, the constant-rate compression tests were conducted under the condition that $p/p_e < 1.1$.

The data based on the constant-rate test show a linear relation with the C-P cell data and also have a good relationship with the gravitational sedimentation data of Group I in the figures. However, Group II shows enormously higher values of α . In the concentration region of Group I, particles settle freely, being out of contact with one another. In the region of Group II, however, they settle to form partial or entire networks, which increases the friction between the particles and the inner wall of the cylinder. The sedimentation rate decreases accordingly, which means an increase in α value.

The extrapolated line of the data of Group I intersects that obtained from the constant-rate

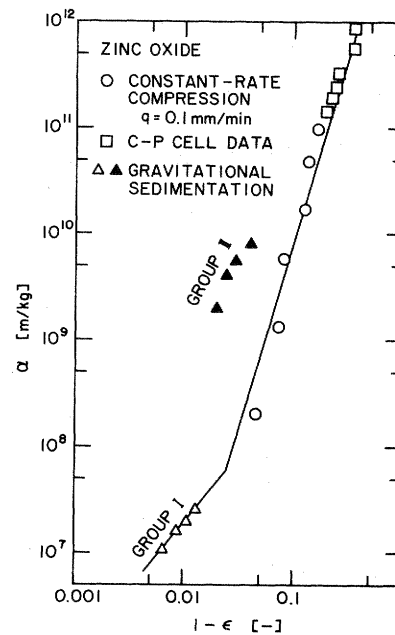


Fig. 9. α vs. $(1-\epsilon)$ for ZnO mixture

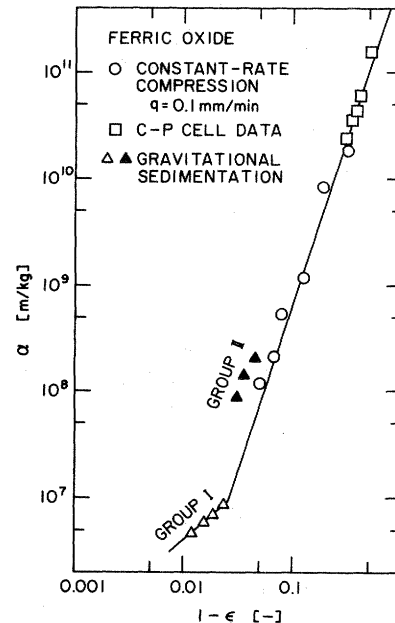


Fig. 10. α vs. $(1-\epsilon)$ for Fe_2O_3 mixture

compression test (at $1-\epsilon=0.024$ in Fig. 9 and 0.026 in Fig. 10). It should be noted that the solidosity at the transition point from Group I to Group II agrees approximately with that at the intersection. In general, these fine particles naturally aggregate to form bigger ones. At the intersection, the aggregates probably contact one another and begin to break up.

Thus, combining the gravitational sedimentation test, the C-P cell test and the constant-rate compression method, one can obtain the permeability characteristic of a solid-liquid mixture in a very wide concentration region, and this is usable to recognize

the separation characteristics of the mixture in fields such as coagulation and flocculation.

Conclusions

The centrifugal sedimentation method and the constant-rate compression method for obtaining compression-permeability characteristics in the intermediate concentration region between gravitational sedimentation data and C-P cell data have been described.

1. By choosing suitable centrifugal acceleration and amount of solid mass, the compression data in the intermediate region can be obtained. These data are in good agreement with those in the concentrated region. However, because of the friction between the inner wall of the cylinder and the sediments investigated, the sedimentation data have a lower solidosity than the values extrapolated from the others.

2. The compression rate at which the internal condition of a compressed mixture is approximately homogeneous can be determined by depicting the relation among p , $(-\Delta e_{av})$ and $(-\omega_0^2/i^2 \cdot de_{av}/d\theta'_c)$. The α -value based on this method can be combined well with C-P cell data and the gravitational sedimentation data for an extremely dilute suspension.

Nomenclature

C_c	= empirical constant in Eq. (4-b)	[—]
C_e	= average modified consolidation coefficient defined by Eq. (14)	[m ² /s]
E	= empirical constant in Eq. (4-a)	[Pa ^{-β}]
e	= local void ratio	[—]
$e_{1,av}$	= initial average void ratio of the mixture	[—]
e_0	= empirical constant in Eq. (4-b)	[—]
i	= number of drainage surfaces	[—]
N	= rotational speed	[1/s]
p	= applied pressure	[Pa]
p_s	= local solid compressive pressure	[Pa]
$p_{s,av}$	= average p_s value	[Pa]
$p_s(e_{1,av})$	= solid compressive pressure corresponding to $e_{1,av}$	[Pa]
R	= distance between center of centrifuge and bottom of sediment	[m]
r	= radial coordinate of cylindrical coordinate system	[m]

r_i	= distance from center of centrifuge to surface of sediment	[m]
α	= local specific resistance	[m/kg]
α_{av}	= average value of α	[m/kg]
β	= empirical constant in Eq. (4-a)	[—]
ε	= local porosity	[—]
θ_c	= consolidation time in constant-rate expression	[s]
θ'_c	= consolidation time in constant-pressure expression	[s]
ρ	= density of liquid	[kg/m ³]
ρ_s	= true density of solid	[kg/m ³]
Ω	= angular velocity	[rad/s]
ω	= net solid volume per unit medium area lying from the medium up to an arbitrary position in the material	[m]
ω_0	= total solid volume in the mixture per unit sectional area	[m]

Literature Cited

- 1) Banks, P. J. and D. R. Burton: submitted to the Editor of *Drying Technology*.
- 2) Buscall, R.: *Colloids and Surface*, **5**, 269 (1982).
- 3) Grace, H. P.: *Chem. Eng. Prog.*, **49**, 303, 367 (1953).
- 4) Murase, T., E. Iritani, J. H. Cho, S. Nakanomori and M. Shirato: *J. Chem. Eng. Japan*, **20**, 246 (1987).
- 5) Murase, T., M. Iwata, I. Kato, W. D. Lee and M. Shirato: *J. Chem. Eng. Japan*, **21**, 204 (1988).
- 6) Sambuichi, M., H. Nakakura, T. Miyoshi and K. Osasa: Preprints of the 53rd Annual Meeting of the Soc. of Chem. Engrs., Japan, Sendai, 254 (1988).
- 7) Schwartzberg, H. G., J. R. Rosenau and G. Richardson: *AIChE Symp. Ser.*, Vol. 73, No. 163, 177 (1977).
- 8) Shirato, M., H. Kato, K. Kobayashi and H. Sakazaki: *J. Chem. Eng. Japan*, **3**, 98 (1970).
- 9) Shirato, M., T. Murase, M. Negawa and H. Moridera: *J. Chem. Eng. Japan*, **4**, 263 (1971).
- 10) Shirato, M.: "Kagaku Kogaku Binran," 4th ed., Maruzen, p. 1140 (1978).
- 11) Shirato, M., T. Murase, E. Iritani and N. Hayashi: *Filtration & Separation*, **20**, 404 (1983).
- 12) Shirato, M., M. Iwata, M. Wakita, T. Murase and N. Hayashi: *J. Chem. Eng. Japan*, **13**, 1 (1987).
- 13) Taylor, D. W.: "Fundamentals of Soil Mechanics," John Wiley & Sons, p. 217 (1962).
- 14) Tiller, F. M. and H. Cooper: *AIChE Journal*, **8**, 445 (1962).

(Presented at Gifu Meeting of The Society of Chemical Engineers, Japan, at Gifu, July, 1988.)